

Generation of size-controlled gold(0) and palladium(0) nanoclusters inside the nanoporous domains of gel-type functional resins

Part I: Synthetic aspects and first catalytic data in the liquid phase

Benedetto Corain^{a,*}, Claudio Burato^b, Paolo Centomo^b, Silvano Lora^c,
Wolfgang Meyer-Zaika^d, Günter Schmid^d

^a C.N.R., Sezione di Padova, c/o Dipartimento di Scienze Chimiche, Istituto di Scienze e Tecnologie Molecolari, via Marzolo 1, 35131 Padova, Italy

^b Dipartimento di Scienze Chimiche, via Marzolo 1, 35131 Padova, Italy

^c Istituto per la Sintesi Organica e la Fotoreattività, C.N.R., Via dell'Università 1, 35020 Legnaro PD, Italy

^d Institut für Anorganische Chemie, Universität Duisburg-Essen, Universitätstrasse 5-7, Essen, Germany

Received 21 May 2004; received in revised form 25 August 2004; accepted 25 August 2004

Available online 12 October 2004

Abstract

The functional resin poly-MTEMA–DMAA–MBA (MTEMA, 2-(methylthio)ethylmethacrylate; 4 mol%, DMAA, *N,N*-dimethylacrylamide, 88 mol%; MBA, *N,N'*-methylenebisacrylamide, 8 mol%) referred to as MTEMA–DMAA–4–8, behaves as a macromolecular ligand towards Pd^{II} and Au^{III} in water (Pd) and acetonitrile (Au). Mⁿ/resin complexes are easily reduced with NaBH₄ in water to M⁰/resin composites. The swollen polymer framework of MTEMA–DMAA–4–8 is seen to act as a “mold” leading to the production of ca. 2.5 nm nanoclusters for both elements. M⁰/MTEMA–DMAA–4–8 composites exhibit useful catalytic properties in various chemical transformations, under mild conditions in water.

© 2004 Elsevier B.V. All rights reserved.

Keywords: Functional resins; Pd⁰ and Au⁰ composites; Metal nanoclusters size versus support nanoporosity

1. Introduction

The production and dispersion of metal nanoclusters onto inorganic supports and amorphous carbon rests on well consolidated technologies belonging to the realm of industrial catalysis and of basic catalysis research [1]. In spite of the existence of a variety of specific synthetic strategies, their very rationale relies on three main approaches, i.e.:

A: precursors of both the metal nanoparticles and of the relevant supports (or the support itself) are intimately mixed under ambient conditions and then thermo-reduced according to very controlled protocols [2];

B: precursors of metal nanoclusters are let to be adsorbed onto suitable supports from the gas or liquid phase and subsequently thermally decomposed [3];

C: metastable size-controlled metal nanoclusters are previously generated in a liquid medium upon reducing a suitable metal precursor, and subsequently transferred onto pre-formed support particles [4].

As to point C, the generation of metastable metal nanoclusters in solution appears to be the so far most investigated and rationalized approach to size-controlled metal nanoclusters in solution. Among the employed stabilizers, linear polymers have been particularly investigated and exploited in the last two decades [5] after the appearance of the seminal paper by Irai in 1979 [6]. With the aim of stabilizing the colloidal systems towards nanoclusters aggregation and to making them meet technological needs, their transfer to the surface of the

* Corresponding author. Tel.: +39 049 8275211; fax: +39 049 8275223.
E-mail address: benedetto.corain@unipd.it (B. Corain).

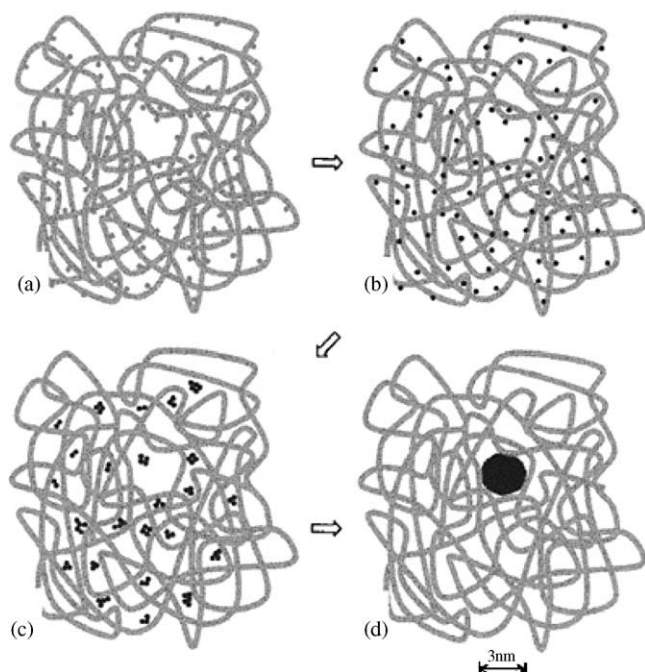


Fig. 1. Generation of size-controlled metal nanoparticles inside metallated resins: our Template Controlled Synthesis approach, TCS). Macromolecular chains are interconnected by cross-linking short chains (not shown in the sketch). Figure depicts a two-dimensional section of a spheroidal volume element ca. 20 nm in diameter. (a) Pd^{II} is homogeneously dispersed inside of the polymer framework; (b) Pd^{II} is reduced to Pd⁰; (c) Pd⁰ atoms start to aggregate in subnanoclusters; (d) a single 3 nm nanocluster is formed and “blocked” inside the largest mesh present in that “slice” of polymer framework. (From ref [19b]).

particles of heterogeneous supports was successfully pursued by a number of authors [7–14].

In the frame of our long lasting interest for the chemical, nanostructural and physico-chemical properties of gel-type resins [15–20], we started to consider their polymer frameworks as a sort of structurally tunable mold in order to obtain size-controlled Pd⁰ nanoclusters directly inside of the body of the individual resins beads. We published our first encouraging results in 2000 [17], in 2003 [19a] that were based on the employment of designed resins of known nanoporosity and, finally, in 2004 [19b] when we established an unquestionable correlation between resin nanoporosity and Pd⁰ nanoclusters size, determined with two quite unrelated techniques, i.e. TEM and XRD-Riedvelt.

Time was mature to test our TCS (Template Controlled Synthesis) approach (Fig. 1) [19b] to another nanostructured metal center, i.e. Au⁰, for which size-control is particularly important in gas-phase reactions [3]. Thus, Au⁰ supported on metal oxides [2] and on carbon [4] is known to be very effective in promoting the catalytic oxidation and hydrogenation of diverse organic substrate in water, or methanol under quite mild conditions [21]. Inspection of the literature [21] reveals that Au⁰ nanoclusters size does not seem to be so dramatically important under liquid phase conditions as it is in gas phase reactions. However, in the frame of the current tumultuous evolution of the knowledge on Au⁰ catalytic chemistry, the viable control of gold nanoclusters size also in catalysts specifically aimed at working in the liquid phase appears to be a relevant issue. In this connection, usefulness of control of metal nanoclusters size is suggested by preliminary results recently provided by Rossi and co-workers [22].

We report in this paper on the synthesis of M⁰/resin (M⁰ = Au⁰, Pd⁰) catalysts (resin = poly-2-(methylthio)ethyl methacrylate-*N,N*-dimethylacrylamide-*N,N'*-methylenebisacrylamide, 4, 8, 88 mol%, Fig. 2), hereafter referred to as MTEMA–DMAA-4–8, with the precise aim of testing our TCS approach to two different metal centers inside of the same nanostructurally characterized functional resin. Preliminary catalytic tests will be also outlined.

2. Experimental

2.1. Apparatus

XRMA: Cambridge Stereoscan 250 EDX PW 9800. TEM: PHILIPS CM 200 FEG with a Supertwin-Lens operated at an accelerating voltage of 200 KeV. Lens parameters: $f = 1.7$ mm, $C_s = 1.2$ mm, $C_c = 1.2$ mm, giving a point resolution of 0.24 nm and a line resolution of 0.1 nm. ISEC: home-assembled apparatus made available by Dr. K. Jerabek, Institute of Chemical Process Fundamentals, Czech Academy of Sciences (Prague-Suchdol). Basic operations and choice of steric probes are described in [23–25].

Samples preparation for TEM: some samples were obtained by mechanical milling of the as-prepared solid sample and subsequent dispersing in ethanol with a ultrasonic bath for 0.5 h. One drop of the so obtained suspension was brought

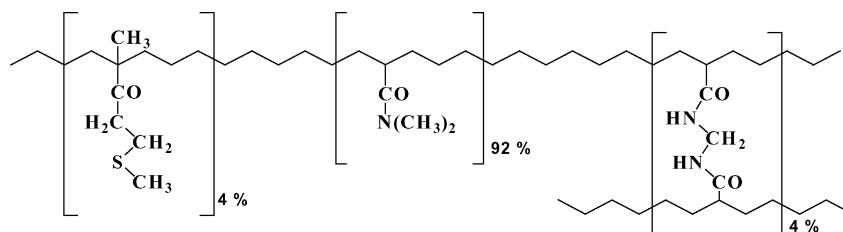


Fig. 2. Primary structure of resin MTEMA–DMAA-4–8.

Table 1
Details on the synthesis and on experimental elemental composition of resin MTEMA–DMAA–4–8

Code	Monomers (g)	C (%)	H (%)	N (%)	S (%)
MTEMA–DMAA–4–8	MTEMA (0.81) DMAA (11.12) MBAA (1.57)	56.65	8.87	13.16	1.39 (0.38) ^a

DMAA = *N,N*-dimethylacrylamide; MTEMA = 2-(methylthio)ethyl methacrylate; MBAA = *N,N'*-methylenebisacrylamide.

^a mmol/g of MTEMA.

onto a carbon-coated copper grid, dried at room temperature and then put into the microscope. Some samples were obtained by embedding the material in Araldite CY212 and, after polymerization, by cutting 70 nm slices with a Diamond-knife.

2.2. Solvents and chemicals

From various commercial sources, used and received.

2.3. Syntheses

The procedure for synthesizing functional resins has been carefully described in ref. [18]. The only difference was in the thorough washing of the crude and ground resins (sieved to 180–400 μm) with methanol in a Soxhlet apparatus for four days. Specific details are collected in Table 1.

Elemental analyses listed in Table 2 are very close to the composition expected from Table 2 (next Section), for a 100% yield, after accounting for absorbed water (from 5.0 to 5.5%).

2.4. Metalation of MTEMA–DMAA–4–8 and reduction to M^0 /resin composites (typical procedure)

The functional resin (ca. 1 g, ca 0.4 mmol –SMe) is suspended in the required medium (see below) and left under moderate stirring for 2 h. Ca. 20 mg (0.06 mmol) of AuCl_3 or ca. 25 mg (0.11 mmol) of $[\text{PdCl}_4]^{2-}$ dissolved in 40 ml MeCN (Au) or water (Pd) are added under manual stirring and left under moderate mechanical stirring for ca. 4 days,

Table 2
Designed composition and observed polymerisation yield of resin MTEMA–DMAA–4–8

Code	Monomer composition	Mol (%)	Polymerisation yield (%)
MTEMA–DMAA–4–8	DMAA MTEMA MBAA	88 4 8	99

DMAA = *N,N*-dimethylacrylamide; MTEMA = 2-(methylthio)ethyl methacrylate; MBAA = *N,N'*-methylenebisacrylamide.

after which time the supernatant phase turns out to be colourless. The resin colour does not appreciably change in the case of Au and it turns to pale brown in the case of Pd. Metalated resins are filtered, washed with water and dried in vacuo at 60 °C to constant weight.

2.5. Reduction of metalated resin in water (typical procedure)

The metalated resin (ca. 1.2 g) is suspended in ca. 200 ml water and left under moderate stirring for 2 h. Ca. 250 mg (6.6 mmol) of NaBH_4 dissolved in 50 ml water are added under manual stirring with consequent vigorous gas evolution and left under moderate mechanical stirring for ca. 90 min. After this time the supernatant phase appears to be colourless and the resins have become burgundy red (Au) and black (Pd). Reduced resins are filtered, washed with water and dried in vacuo at 60 °C to constant weight.

3. Results and discussion

The designed resin is aimed at possessing pendants able to covalently link Pd^{II} and Au^{III} ions, i.e. thioetheral units. Moreover, the resin is featured by a moderate cross-linking degree as it is requested to give a gel-type resin and by an essentially amphiphilic character [20a,c,h]. Resin design and composition and relevant polymerisation yield are reported in Table 2.

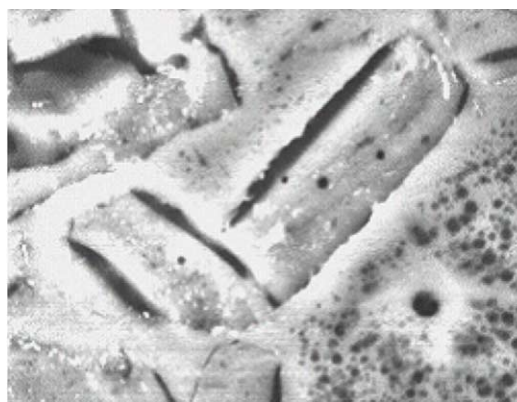
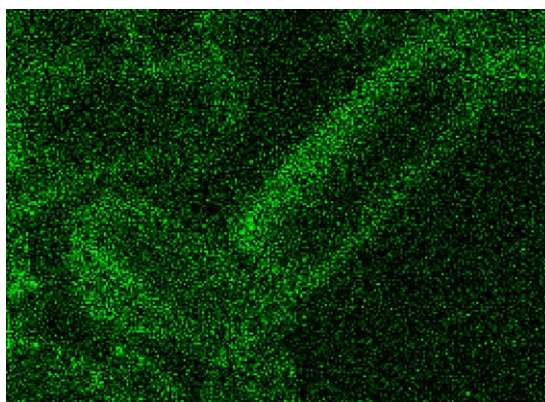


Fig. 3. XRMA scanning picture of Pd/MTEMA–DMAA–4–8 (left) and SEM picture of the relevant section (right).

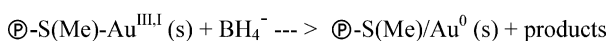
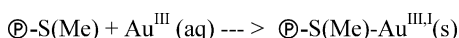
Table 3
Data for Au⁰, Pd⁰/resin composites

Code	Au (%)	Pd (%)	Colour
MTEMA–DMAA–4–8	0.75	0.70	Burgundy red (Au) Black (Pd)

Quite in line with our long-standing experience [20e,h], co-polymerization of the employed monomers and cross-linker promoted by γ -rays leads to the facile and quantitative conversion to the desired materials bearing ca. 0.4 mmol/g of thiomethyl functionality (Fig. 2). Resins are obtained as 180–400 μ m brittle colorless and transparent particles (see Experimental) with a reasonable swellability in water and methanol (2–3 ml/g).

As anticipated above, the choice of monomer 2-(methylthio)ethyl methacrylate (MTEMA) was suggested by the reasonable expectation that the thioetheral functionality should be a useful ligating site for anchoring Au^{III} to the functional resin and as a means of homogeneous dispersion of the metal centers (and consequently of Au⁰ nanoclusters, Fig. 1) through the body of the resin particles in the synthetic steps 1–2. The thioetheral functions are also useful as stabilizing sites for the Au⁰ nanoclusters thus counteracting sintering trends.

In fact, the resin reacts easily with AuCl₃ in MeCN and with Pd(OAc)₂ in THF/H₂O 2:1 to give colourless and light brown materials respectively, which are subsequently reduced with NaBH₄ in water to give red (Au) and black (Pd) materials, respectively (Table 3), i.e.:



3.1. MTEMA–DMAA–4–8

MTEMA–DMAA–4–8 was analysed with ISEC (Inverse Steric Exclusion Chromatography) [24,26] in water and relevant resin/M⁰ composites were characterised with XRMA and with TEM. ISEC provides accurate information on the nanometer scale morphology of a given resin, after its swelling in a convenient liquid medium. It is based on measurements of elution behaviour of standard solutes with known effective molecular size that are let to flow through a column filled with the investigated material under conditions in which the elution is influenced exclusively by the (nano)morphology of the stationary phase. Similarly to the case of the other porosimetric methods, mathematical treatment of the elution data allows one to obtain information on the morphology of the investigated material using a simple geometrical model. It is now established that for describing the morphology of swollen polymer gels the best suitable tool is the so-called Ogston's model [25] that depicts pores as spaces between randomly oriented solid rods. This geometry, albeit a fair simplification of the morphology of swollen

polymer networks, provides a faithful description of both the intensive parameters (polymer chain densities) and extensive properties (specific volumes of variously dense polymer fractions). On the other hand, the conventional model of the so-called cylindrical pores [26] relies on a geometry that is not directly related to the physical reality of the polymer framework but that can be used, from the mathematical point of view, for correlating the chromatographic data to the morphology of the polymer framework at the nanometer scale with essentially the same accuracy provided by Ogston's model. As a matter of fact, the porosity of a swollen gel described upon using cylindrical pore geometry gives easily understandable information about effective size of the cavities among the polymer chains although the specific pore volume data per se might be somewhat erroneous. However, for investigating on the factors affecting the formation of metal nanoclusters inside of the swollen polymer matrix, the effective size of the "cavities" used in the templating molds is much more important than their specific volume.

Results of ISEC characterisation of the swollen state morphology in water of MTEMA–DMAA–4–8 resins are conveniently illustrated in Table 4.

The resin appears to be built up with domains predominantly featured by 0.5 and 2.5 nm "cylindrical pores". Consequently, if the model illustrating the TCS strategy (Fig. 1) is correct, we expect the predominant formation of ca. 2.5 nm M⁰ nanoclusters.

3.2. XRMA analysis

In the frame of our endeavour for the designed synthesis of M⁰/resin nanocomposites [15–20], we normally take advantage of X-ray Microprobe Analysis (XRMA) to monitor the location of the produced metal nanoclusters ("scanning picture" mode) in the body of the catalyst particles that are normally just submillimetric in size. This convenient technique is featured by a ca. 5 μ m practical resolution power and provides a useful view of metal distribution normally

Table 4
ISEC characterisation of the macromolecular template MTEMA–DMAA–4–8

	MTEMA–DMAA–4–8
Sample wt. (g)	1.54
Dead volume (ml)	1.22
Pore diameter (nm)	(ml/g)
0.5	2.17
1	0
2.2	0.19
2.5	0.79
2.7	0.01
3.2	0.04
3.5	0.06
4	0
Average pore diameter (nm)	2.5

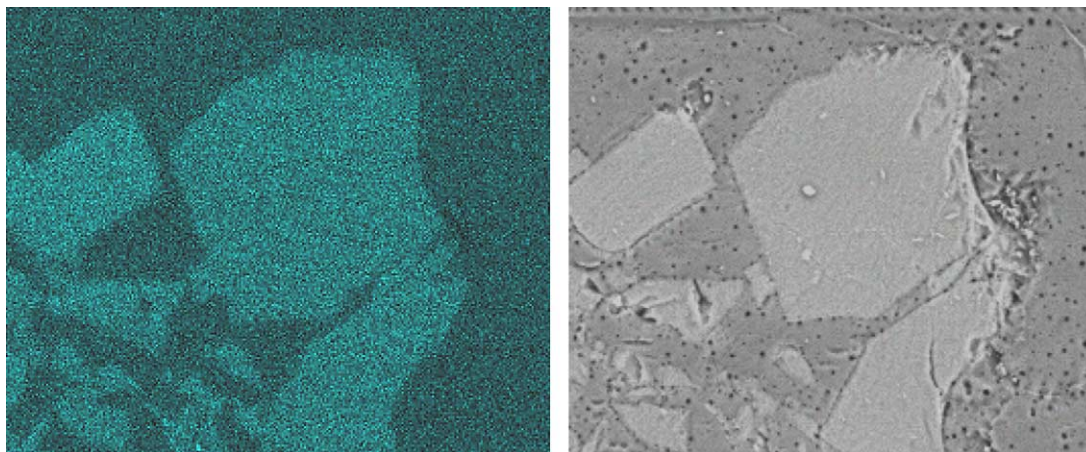


Fig. 4. XRMA scanning picture of Au/MTEMA-DMAA-4-8 (left) and SEM picture of the relevant section (right).

through equatorial sections of the metalated resins particles (Figs. 3 and 4).

It is seen that metal nanoclusters dispersion through the body of the support is homogeneous in the case of Au^{III} and somewhat peripheral in the case of Pd^{II}.

3.3. TEM analysis

Pd⁰ and Au⁰ are present as well spaced narrowly size-dispersed spheroidal nanoparticles (Figs. 5 and 6).

The relevant nanoclusters diameters are compared in Table 5 with the predominant largest pores observed by ISEC analysis in the resin framework (see Fig. 1).

The agreement between the expected and the observed size of the metal nanoclusters is complete in accordance with the TCS model [19b]. A perceivable size increase of Pd⁰

nanoclusters is observed with the aging of the metal/resin composite in the laboratory atmosphere and the effect is more marked in the case of Au⁰. Apparently, this phenomenon deserves further thorough investigation.

3.4. Catalytic tests

The Au⁰/resin composite described in this paper is the second example of resin-supported Au⁰ potential catalyst. In fact, Shi and Deng [27] recently reported on a rather ill defined material obtained upon impregnation of the macroreticular resin Ionexchanger IV (Merck, Darmstadt, Germany) with aqueous HAuCl₄. The authors do not provide information on metal distribution through the resins particles, stating that the catalyst contains Au⁰ and that “average size of the Au⁰ nanoparticles is less than 10 nm” [27]. In spite of

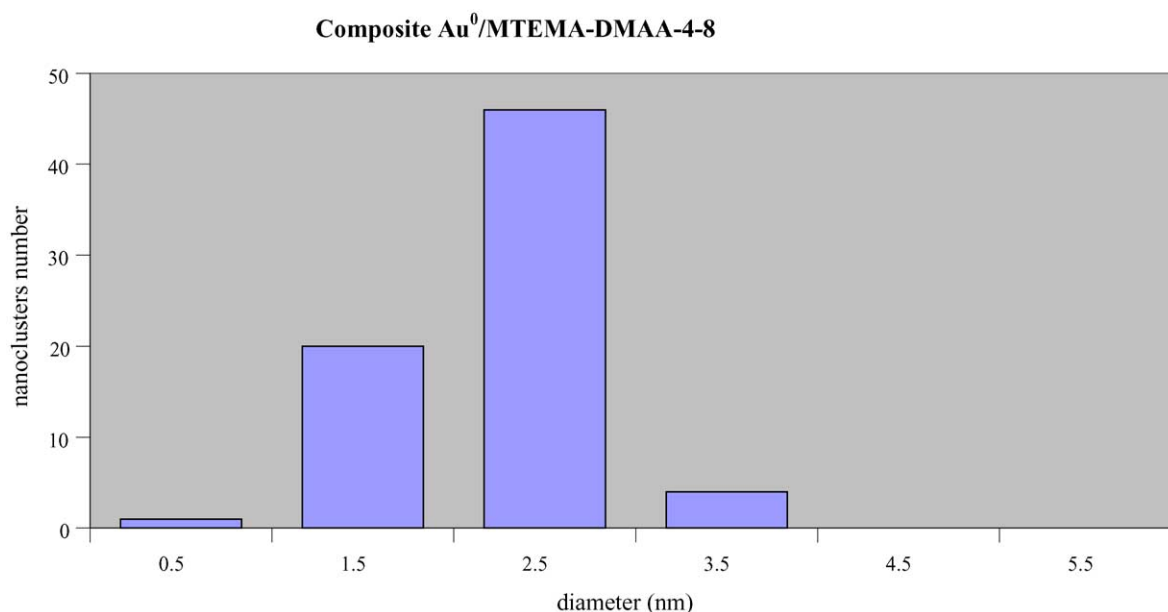


Fig. 5. Size distribution of the metal nanoclusters in the Au⁰/MTEMA-DMAA-4-8 catalyst.

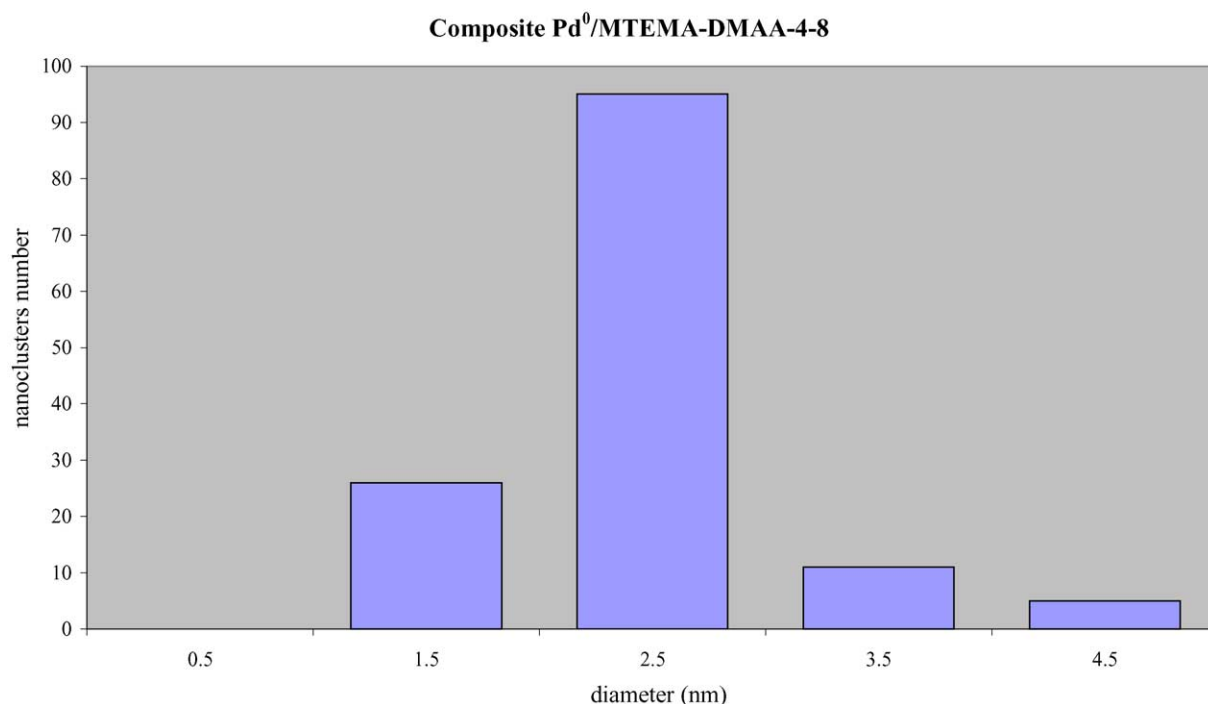


Fig. 6. Size distribution of the metal nanoclusters in the Pd⁰/MTEMA–DMAA–4–8 catalyst.

Table 5

Predominant largest pores diameter in MTEMA–DMAA–4–8 vs. observed average nanoclusters diameter in M⁰/MTEMA–DMAA–4–8 catalysts (M = Au, Pd)

Predominant largest pores	2.5 nm
Average nanoclusters (Au)	2.2 nm ^a
Average nanoclusters (Pd)	2.3 nm ^b

^a 3.3 nm after 6 months storage.

^b 2.6 nm after 12 months storage.

this paucity of pieces of information, their catalyst appears to be quite interesting in that it is remarkably active in the oxidative carbonylation of amines to carbamates and substituted ureas at 175 °C. It is worth noting that the actual operational conditions are rather unusual in that they start under liquid phase conditions with no added solvent, and they end up a solid phase (the liquid phase is eventually totally consumed).

We have started a series of catalytic tests aimed at surveying the catalytic efficiency of our catalyst in three significant systems: (a) oxidation of *n*-aldehydes to *n*-carboxylic acids with molecular oxygen in water (a model reaction) [28], (b) oxidation of *n*-butanol to *n*-butanal again with dioxygen in water [29] and (c) the direct synthesis of hydrogen peroxide from dihydrogen and dioxygen under quite mild conditions in a water–methanol mixture [30]. All tests are successful and we anticipate here a few preliminary results relevant to point (a). A full collection of catalytic results will be presented in Part II [31] together with the description of the synthesis and characterization of other resins-based Au⁰ and Pd⁰ catalysts closely related to Au⁰/MTEMA–DMAA–4–8.

3.5. Pentanal oxidation to pentanoic acid

Catalyst Au⁰/MTEMA–DMAA–4–8 was tested in water at 70 °C, P_{O₂} = 3 atm, [K₂CO₃] = 0.23 M. The results obtained after 2 h, for aldehyde/cat. molar ratio equal to 1000, reveal that the new catalyst is twice as active as a classic Au⁰/C one. Thus, the conversion of pentanal into pentanoic acid was equal to 95% to be compared with 42% observed with Au⁰/C, under identical conditions [31].

4. Conclusions

A moderately cross-linked co-polymer of *N,N*-dimethylacrylamide, 2-(methylthio)ethyl methacrylate and *N,N*-methylenebisacrylamide proves to be an effective macromolecular ligand able to extract upon co-ordination Pd^{II} and Au^{III} from water and acetonitrile solutions, respectively, and to thoroughly disperse them inside of its polymer framework. Chemical reduction with NaBH₄ in water leads to M⁰/resin composites, in which a good size-control of the generated metal nanoclusters, 2.2 nm (Au) and 2.3 nm (Pd), is observed. Catalyst Au/MTEMA–DMAA–4–8 is active in water in the oxidation of pentanal to pentanoic acid by dioxygen under mild conditions.

Acknowledgements

This work was partially supported by P.R.I.N. funding 2001–2003, Ministero dell'Università e della Ricerca Scien-

tifica, Italy (Project number 2001038991). We are indebted to Dr. K. Jerabek for his supervision to one of us (CB) in Prague and with Company “Programma Ambiente”, Padova, Italy for timely and accurate performing of Au and Pd elemental analyses. We are also indebted to Prof. L. Prati for communicating some preliminary catalytic results obtained in her laboratories with our materials and to Dr. L. Tauro and to Dr. M. Favaro for careful performing of XRMA. Alexander von Humboldt Foundation is gratefully acknowledged for a Wiederaufnahme Scholarship provided to one of us (B.C.).

References

- [1] (a) G. Ertl, H. Knötzinger, J. Weitkamp, Handbook of Heterogeneous Catalysis, Jossey-Bass, New York, 1997;
(b) E. Gallei, E. Schwab, Catal. Today 51 (1999) 535.
- [2] S. Schimpf, M. Lucas, C. Mohr, U. Rodemerk, A. Brückner, J. Radnik, H. Hofmeister, P. Claus, Catal. Today 72 (2002) 63, and references therein.
- [3] (a) M. Haruta, CATTECH 6 (2002) 102, and references therein ;
(b) A. Wolf, F. Schüth, Appl. Cat. A: Genera 226 (2002) 1, and references therein.
- [4] (a) S. Biella, L. Prati, M. Rossi, J. Catal. 206 (2002) 242, and references therein ;
(b) C.L. Bianchi, S. Biella, A. Gervasini, L. Prati, M. Rossi, Catal. Lett. 85 (2003) 91, and references therein.
- [5] T. Teranishi, M. Miyake, Chem. Mater. 10 (1998) 594, and references therein.
- [6] H. Hirai, J. Macromol. Sci. Chem. A13 (1979) 633.
- [7] N. Toshima, T. Teranishi, H. Hasanuma, Y. Saito, J. Phys. Chem. 96 (1992) 3796.
- [8] T. Teranishi, N. Toshima, J. Chem. Soc. Dalton Trans. (1994) 2967.
- [9] T. Teranishi, N. Toshima, J. Chem. Soc. Dalton Trans. (1995) 979.
- [10] S.J. Tauster, Acc. Chem. Res. 20 (1987) 387.
- [11] K. Sayo, S. Deki, S. Hayashi, Eur. Phys. J. D9 (1999) 429.
- [12] A.B.R. Mayer, Mater. Sci. Eng. C6 (1998) 155.
- [13] M.K. Corbierre, N.S. Cameron, M. Sutton, S.G.J. Mochrie, L.B. Lurio, A. Rühm, R.B. Lennox, J. Am. Chem. Soc. 123 (2001) 10411.
- [14] J. Lee, V.C. Sundar, J.R. Heine, M.G. Bawendi, K.F. Jensen, Adv. Mater. 12 (2000) 1102.
- [15] M. Kralik, M. Hronec, S. Lora, G. Palma, M. Zecca, A. Biffis, B. Corain, J. Mol. Catal. 97 (1995) 145.
- [16] M. Kralik, V. Kratky, P. Centomo, P. Guerriero, S. Lora, B. Corain, J. Mol. Catal. A: Chem. 195 (2003) 211.
- [17] A. Biffis, A.A. D’Archivio, K. Jerabek, G. Schmid, B. Corain, Adv. Mater. 12 (2000) 1909.
- [18] M. Kralik, V. Kratky, M. De Rosso, M. Tonelli, S. Lora, B. Corain, Chem. Eur. J. 9 (2003) 209.
- [19] (a) F. Artuso, A.A. D’Archivio, S. Lora, K. Jerabek, M. Kralik, B. Corain, Chem. Eur. J. 9 (2003) 5292;
(b) B. Corain, K. Jerabek, P. Centomo, P. Canton, Angew. Chem. Int. Ed. 43 (2004) 959.
- [20] (a) A. Biffis, B. Corain, M. Zecca, C. Corvaja, K. Jerabek, J. Am. Chem. Soc. 117 (1995) 1603;
(b) M. Zecca, A. Biffis, G. Palma, C. Corvaja, S. Lora, K. Jerabek, B. Corain, Macromolecules 29 (1996) 4655;
(c) A.A. D’Archivio, L. Galantini, A. Panatta, E. Tettamanti, B. Corain, J. Phys. Chem. B. 102 (1998) 6779;
(d) B. Corain, M. Kralik, J. Mol. Catal. A: Chem. 159 (2000) 153;
(e) B. Corain, M. Kralik, J. Mol. Catal. A: Chem. 173 (2001) 99;
(f) B. Corain, M. Zecca, K. Jerabek, J. Mol. Catal. A: Chem. 177 (2001) 3;
(g) A. Biffis, R. Ricoveri, S. Campestrini, M. Kralik, K. Jerabek, B. Corain, Chem. Eur. J. 8 (2002) 2962;
(h) B. Corain, P. Centomo, S. Lora, M. Kralik, J. Mol. Catal. A: Chem. 204-205 (2003) 755–762;
(i) B. Corain, P. Guerriero, G. Schiavon, M. Zapparoli, M. Kralik, J. Mol. Catal. A: Chem. 211 (2004) 237.
- [21] G. Schmid, B. Corain, Eur. J. Inorg. Chem. (2003) 3081 (review paper).
- [22] F. Porta, L. Prati, M. Rossi, S. Coluccia, G. Martra, Catal. Today 61 (2000) 165.
- [23] M. Kralik, M. Hronec, V. Jorik, S. Lora, G. Palma, M. Zecca, A. Biffis, B. Corain, J. Mol. Catal. A: Chem. 101 (1995) 143.
- [24] (a) K. Jerábek, Anal. Chem. 57 (1985) 1595;
(b) K. Jerábek, Anal. Chem. 57 (1985) 1598.
- [25] A.G. Ogston, Trans. Faraday Soc. 54 (1958) 1754.
- [26] K. Jerabek, in: Cross Evaluation of Strategies in Size-Exclusion Chromatography, M. Potschka, P.L. Dubin (Eds.), ACS Symposium Series 635, American Chemical Society, Washington, DC, USA, 1996, p. 211.
- [27] F. Shi, Y. Deng, J. Catal. 211 (2002) 548.
- [28] S. Biella, L. Prati, M. Rossi, J. Mol. Catal. A: Chem. 197 (2003) 207.
- [29] Y. Uozumi, R. Nakao, Angew. Chem. Int. Ed. 42 (2003) 194.
- [30] P. London, P.J. Collier, A.J. Papworth, C.J. Kiely, G.J. Hutchings, Chem. Commun. (2002) 2058.
- [31] C. Burato, P. Centomo, M. Favaro, G. Pace, W. Meyer-Zaika, G. Schmid, L. Prati, B. Corain, J. Mol. Catal. A: Chem., in preparation.